International Journal of Mechanical, Industrial and Aerospace Sciences
ISSN: 2517-9950
Vol:6, No:12, 2012

Laminar Impinging Jet Heat Transfer for Curved Plates

A. M. Tahsini, and S. Tadayon Mousavi

***Abstract*—**The purpose of the present study is to analyze the effect of the target plate's curvature on the heat transfer in laminar confined impinging jet flows. Numerical results from two dimensional compressible finite volume solver are compared between three different shapes of impinging plates: Flat, Concave and Convex plates. The remarkable result of this study proves that the stagnation Nusselt number in laminar range of Reynolds number based on the slot width is maximum in convex surface and is minimum in concave plate. These results refuse the previous data in literature stating the amount of the stagnation Nusselt number is greater in concave surface related to flat plate configuration.

***Keywords*—**Concave, Convex, Heat transfer, Impinging jet, Laminar flow.

I. Introduction

IMPINGING jets are used in various industrial applications because of producing high heat and mass transfer coefficients. The flow structures of unconfined impinging jets are divided to three main regions: free jet region, stagnation region and wall jet region. The maximum Nusselt number is observed at the stagnation point or the surrounding point due to the formation of thin thermal boundary layer in that region. Confined impinging jets have these three global regions, but the upper wall that is in the same level with nozzle's exit restricts entrainment of jets, so the length of potential core in confined jets is more than free jets; therefore the Nusselt number has experienced greater amount related to free jet in the same condition for laminar impinging jets.

Several investigations have been done on the impinging jets for many years that have been discussed the important factors on such flow structures. Viskanta [1] has gathered a whole and comprehensive review of numerical and experimental researches that had been done before. Gardon and Akfirat [2] have experimentally measured the heat transfer of submerged impinging jets. Chirac and Ortega [3] has numerically studied the heat transfer, flow structures and transitional behaviors of confined slot jet at a fixed nozzle to surface distance and different Reynolds numbers. Park et al. [4] have numerically studied two dimensional laminar and turbulent impinging slot jets using *Simple*-base segregated streamline upwind Petrov-Galerkin finite element method. It has been indicated that this method is more accurate than other upwind numerical methods that used the artificial diffusion. Lee et al. [5] has numerically investigated the flow structures and distribution of the Nusselt number, and pressure coefficient along the flat plate. Lee et al. [6] have experimentally measured the Nusselt number distribution over isothermal flat plate. This study focused on describing unsteady modes for each height ratio and Re number. Rady and Arquis [7] have numerically compared local and stagnation Nusselt number of a multiple impinging slot jets over an isothermal flat plate in laminar regime. They analyzed the effect of exhaust ports and spent flow on heat transfer rates, and they suggested that locating surface protrusions before exhaust ports can be enhanced the Nusselt number and reduce adverse effect of spent flow in multiple impinging jet systems. Kubacki and Dick [8] have numerically investigated the turbulent confined plane impinging jets using different turbulent models. Jaramillo et al. [9] have presented a comprehensive comparison between different k-w and k-ε models with DNS modeling.

All above-mentioned studies are related to the flat impinging plate, although some researches have been done on curve impinging plate. Kayansayan and kucuka [10] both experimentally and numerically have investigated the flow structure and parameters on concave impinging plate. They analyzed turbulent and laminar regimes for confined plane impinging jets that are issued from the symmetry line of semi-cylindrical channel. Measurement of pressure and Nusselt number distribution over impinging plate has been reported. They simulated the laminar flow by a numerical model too. It has been indicated the amount of the Nusselt number over target plate has been enhanced compared to flat plate due to surface curvature. Rahman and Hernandez [11] have numerically studied the conjugate heat transfer between a round water jet and convex surface. In this analysis, a constant heat flux is imposed on the bottom edge of the surface, and consideration of different solid material and plate thicknesses for the convex surface have been given generality to this investigation. Choi et al. [12] have experimentally measured the distribution of mean velocity and fluctuating velocity over a concave surface for turbulent impinging slot jet. They interpreted the measured local and stagnation Nusselt number over the concave plate by turbulent characteristics of flow around stagnation region and wall jet region. Yang et al. [13] have numerically investigated the Nusselt number distribution and velocity field over concave surface for turbulent impinging jet at relatively small curvature. The k-ε model was used for simulation of turbulent jet. Validation with experimental result has been proved the accuracy of this

A. M. Tahsini, Assistant Professor, Aerospace Research Institute, Tehran, Iran; e-mail: a_m_tahsini@yahoo.com.
S. Tadayon Mousavi, M. Sc. Student, Aerospace Research Institute, Tehran, Iran.

model. Cornaro et al. [14] have visualized flow over concave and convex surface at relative high curvature for turbulent impinging round jet. They investigated the effects of nozzle to surface distances, relative curvature and Re number on vortex formation both at the distance between nozzle to surface and in the stagnation region on the wall. A comprehensive comparison for flow structure between free jet, impinging jet upon flat plate and impinging jet upon concave and convex surface has been presented.

As mentioned above, most of the researches have been concerned on turbulent regime for concave or convex impinging surface. In the laminar regime, reference [10] has been stated that the Nusselt number along concave surface has been enhanced with respect to flat plate by destabilization due to centrifugal force. However, flow analysis at the present study has been proved the amount of the Nusselt number must be lower in concave surface than flat plate case, because curvature of concave surface prevents fluid to flow smoothly on the surface; Therefore, Nusselt number has been decreased. Here the numerical simulation of laminar impinging slot jet has been done using finite volume method to prove this claim. In addition, a comprehensive comparison between the Nusselt number at two different laminar Re numbers over convex, concave and flat plates are presented.

II. Governing Equations

Two dimensional compressible continuity, momentum and energy equations are governed flow in this study. The flow transport and thermodynamic properties are assumed constant during solution process. The conservative forms of governing equations are presented below.

Continuity,

$$\frac{\partial \rho}{\partial t}+\frac{\partial}{\partial x_j}(\rho u_j)=0 \tag{1}$$

Momentum,

$$\frac{\partial(\rho u_i)}{\partial t}+\frac{\partial}{\partial x_j}(\rho u_i u_j)=-\frac{\partial P}{\partial x_i}+\frac{\partial}{\partial x_j}(\tau_{ij}) \tag{2}$$

Energy,

$$\frac{\partial(\rho E)}{\partial t}+\frac{\partial}{\partial x_j}(\rho u_j E)=-\frac{\partial}{\partial x_j}(P u_j)+\frac{\partial}{\partial x_j}(\tau_{ij} u_i)+k\frac{\partial^2 T}{\partial x_j{}^2} \tag{3}$$

Simulation is done by employment of the cell center finite volume scheme. Every grid cell is defined as a control volume in this method, and flow properties are stored at the center of the grid. Inviscid and viscous fluxes must be computed at each face of the control volume. Then fluxes are integrated over cell to define flow properties at the center of the control volume. Governing equations are discretized separately in time and space based on the method of lines. Inviscid fluxed is computed based on AUSM$^+$. General form of splitting and computing inviscid fluxes at each face of the control volume is mentioned below, and more details can be found in reference [15].

Green's theorem is used to compute first derivative of velocity's components and temperature at the faces of every grid cell. After the derivatives are computed, viscous fluxes can be calculated at each face. Simple explicit method is employed for discretization in time after the fluxes integrated over the control volume. All above steps with using proper boundary condition are repeated until convergence is achieved in numerical domain. Ghost cells are used to impose proper boundary condition for numerical simulation. At upper and lower wall, no slip condition and constant temperature are imposed, at exit boundary, atmospheric pressure is set, at the jet inlet, uniform velocity and constant temperature is used, and at the symmetry line, the first component of velocity and the first derivative of temperature and pressure are vanished.

To prove correct prediction of the Nusselt number distribution on the impinging plate, a comparison between present and Lee [5] results for impinging jet over flat plate at Re=300 and H/b=2 is shown in Fig. 1. Present results correspond reasonably with Lee results at both cases.

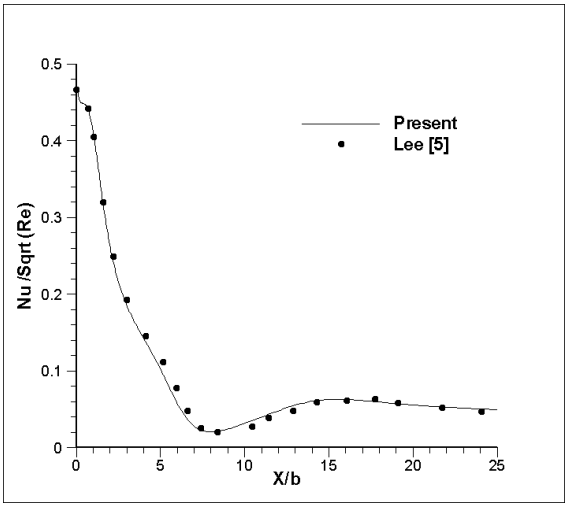

Fig. 1 Nusselt number over impinging flat plat at Re=300 and H/b=2

Fig. 2 shows the computational domain and coordinate system for concave surface as impinging plate. The flow is steady and symmetric with respect to the jet axis at investigated Reynolds numbers 300 and 460 for every studied case, so only half of the impinging plate is considered for solution. The length of the channel in flat plate case is chosen 50b because the length of the re-circulation region both at the lower and upper wall can be completely captured and exit boundary condition cannot affect the domain solution. For the Concave and Convex cases, a channel-like shape is attached to the computational domain after quadrant area is finished so that the results can be compared with results of reference [10].

The length of channel-like shape is chosen in the same manner, as the channel length is determined in the flat plate case. Sequentially, 20 and 15 times greater than nozzle width are chosen for concave and convex channel-like length. The Prandtl number is chosen 0.72 as the same with reference [10]. The curvature is defined as a ratio of confined wall radius to the impinging surface radius for concave cases, so three different curvature ratios 1.5, 2 and 2.5 are considered to investigate the effect of curvature on local and stagnation Nusselt number on target wall. The same impinging wall radius in each curvature ratio case is chosen for convex impinging wall in order to compare the Nusselt number with concave cases. All simulations are done at constant nozzle to surface distance 2.2b.

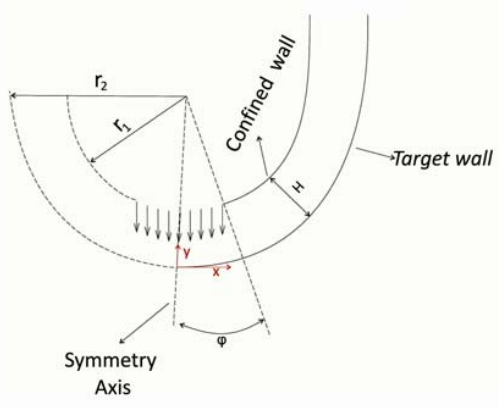

Fig. 2 Computational domain and coordinate system for concave surface as impinging plate

Structured grid is used to divide the computational domain to adequate cells. Fig. 3 shows distribution of Nusselt number on concave impinging plate at Reynolds number 460 and radius ratio 1.5 for three different grid sizes. All of the grid sizes show the same Nusselt number behavior, so it is reasonable to choose the second one, 180 nodes along channel height and 600 nodes along channel width, as independent grid size to implement for other cases. The final results on curvature effect on the heat transfer under impinging jet are presented in a next section.

III. Results and Discussion

Lack of the accurate results and vital contradictions between available results at laminar regime for impinging jet upon curved surface are inspirations to investigate the flow behavior and the Nusselt number distribution at this study, so a comprehensive comparison for different impinging plate curvatures are presented in this section. As mentioned in literature review, one of the rare studies on the flow characteristics at laminar impinging jet over concave surface has been done by Kayansayan [10], but confusing interpretation and results are perceived at this paper.

The Nusselt number distribution over a flat plate, concave plate at radius ratio 1.5 and concave plate at the same radius ratio from Kayansayan[10] at Reynolds number 460 is demonstrated in Fig. 4. Based on Kayansayan's [10] claim, the Nusselt number at stagnation region is enhanced by decreasing curvature, so flat plate as an impinging surface must have higher Nusselt number at stagnation region related to concave surface at any curvatures. Moreover, Lee et al. [5] numerically showed that the critical Reynolds number at which the flow becomes unsteady for H/b=2 is around 350. Based on their study the time averaged stagnation Nusselt number for Re=460 and H/b=2 is around 9.86 that is agreed well with present simulation of stagnation point Nusselt number at this investigative case. Nevertheless, Kayansayan [10] predicted Nusselt number at stagnation region is higher than corresponded flat plate geometry. Therefore, the claim that the Nusselt number has been enhanced in concave plate related to flat plat at laminar regime is a controversial issue. The following comparisons try to demonstrate and prove the correct Nusselt number behavior on curved surfaces at the laminar regime.

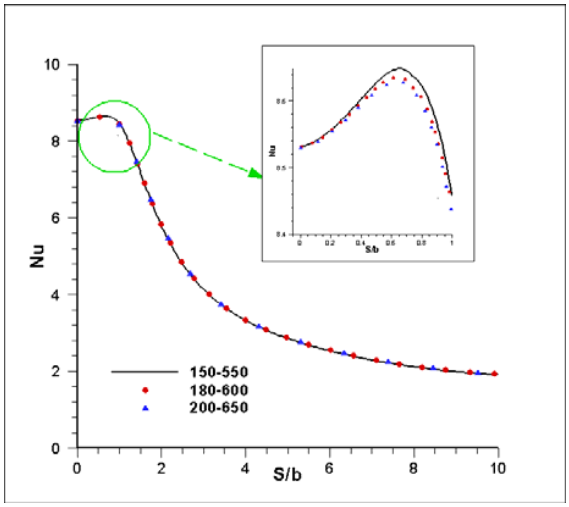

Fig. 3 Local Nusselt number over concave impinging plate at Re=460 and R=1.5

Figs. 5 and 6 show comparison for Nusselt number over a flat plate, concave and convex surfaces sequentially at Re=460 and R=1.5 and Re=300 and R=2. All the simulated cases show the same behaviors, so only two cases are presented to preserve coherence of discussion.

At stagnation region, Nusselt number has the highest value at convex plate and heat transfer at this region is higher at the flat plate case with respect to the concave plate as shown in the both figures. Concave shape does not allow fluid to diffuse easily, or fluid cannot flow smoothly on the surface because of the concave shape resistance. Therefore, the formed boundary layer on the surface is thicker than other cases at stagnation region. On the contrary, convex shape does not resist against fluid motion, so flow passes the surface without any shape restriction, and thermal boundary layer is the thinnest one at convex surface.

This behavior can be explained by the centrifugal force effect on curved plate too. Since this force causes the flow becomes more stable and fluid flows more smoothly on the convex surface in related to the other plate shapes, the formed boundary layer on the surface is thinner at convex plate and consequently Nusselt number is higher than two other cases. Besides, centrifugal force acts oppositely on concave plate; hence the thermal boundary layer is the thickest one specifically at stagnation region and this phenomenon causes low value for the Nusselt number. Distribution of the Nusselt number over flat plate shows behavior that is bounded between concave and convex cases.

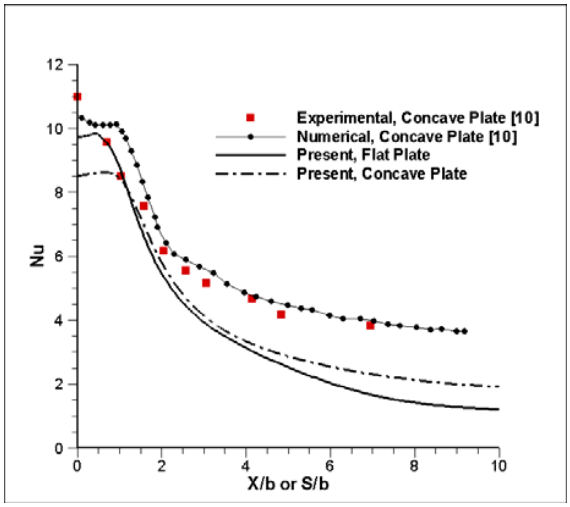

Fig. 4 Comparison of Present Nusselt number and Kayansayan [10] result at Re=460, H/b=2.2, and R=1.5

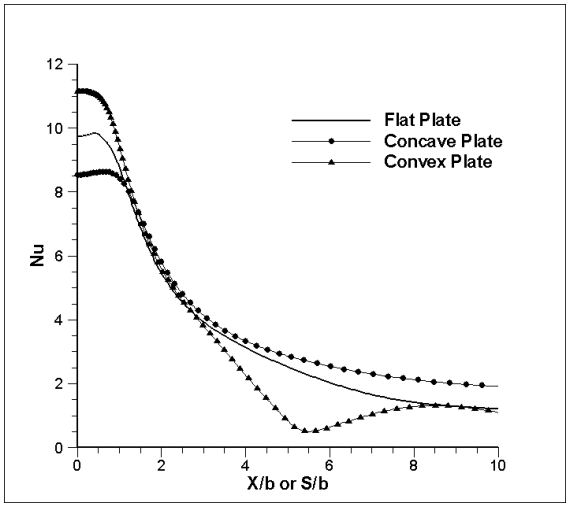

Fig. 5 Comparison for Nusselt number over three different impinging plat shape at Re=460 and R=1.5

Viscous effects are more dominant at lower Reynolds number, so boundary layer thickness is reduced at stagnation region as Reynolds number increases and consequently the Nusselt number is enhanced. This behavior is obvious in Figs. 5 and 6.

Confined impinging plate at laminar regime confronts with two recirculation regions, one of them is at the upper wall and the other is observed at the lower plate. Entrainment of impinging jet forms the first recirculation at the confined plate and its strength is increased at higher Reynolds number. In addition, formation of second recirculation at impinging plate is due to re-entrainment of the wall jet flow to impinging jet and retarding effect of viscous forces on the lower wall. Position and strength of impinging plate recirculation depends on the position of the upper wall recirculation region, Reynolds number, distance of nozzle to impinging plate and impinging plate curvature.

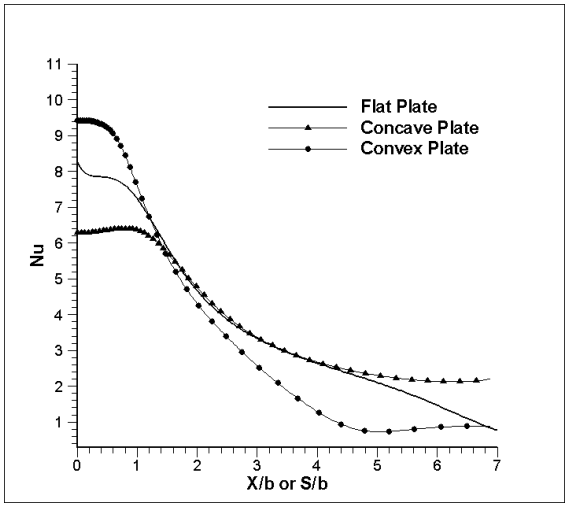

Fig. 6 Comparison for Nusselt number over three different impinging plat shape at Re=300 and R=2

At the downstream of the stagnation region, the Nusselt number decreases for all the cases, but after a local minimum at convex surface, heat transfer increases. This phenomenon can be interpreted by re-circulation region at impingement plate. The enhancement of Nusselt number occurs between separation and re-attachment points of re-circulation region at convex surface.

Figs. 7 and 8 show comparisons for the Nusselt number distribution over concave and convex surfaces at different surface curvatures. It should be mentioned that impinging plate radii for convex surface are chosen equal to corresponded concave cases and dimensionless distance between nozzle and impinging plate with respect to nozzle width is the same for all cases. These two geometrical parameters are enough and essential to compare results for different curvatures. Hence, it is impossible and irrelevant to set same radius ratio at both corresponded concave and convex cases.

As it is expected, Nusselt number at stagnation region is enhanced by decreasing curvature due to thinner formed thermal boundary layer for concave surface. On the other

hand, heat transfer at stagnation region is decreased by decreasing convex plate radius because of thicker boundary layer at stagnation region. In fact, this type of the flow behavior resemble drag coefficient on the curved surface. Since flow cannot diffuse over concave surface more conveniently than convex plate, drag coefficient is higher for concave than convex surface.

At both concave and convex surfaces, the heat transfer diminishes after the stagnation region. In fact, the Nusselt number is lower for higher curvature at downstream of the stagnation region in convex case. On the contrary, the heat transfer is a little more over the concave plate at higher radius ratio after the stagnation region. Based on the above results, it can be concluded that in spite of the pervious interpretation, the curvature affects distribution of the Nusselt number at stagnation region seriously, so consideration of the curvature effects at this region is vital for correct prediction of heat transfer and flow characteristics over curved surfaces.

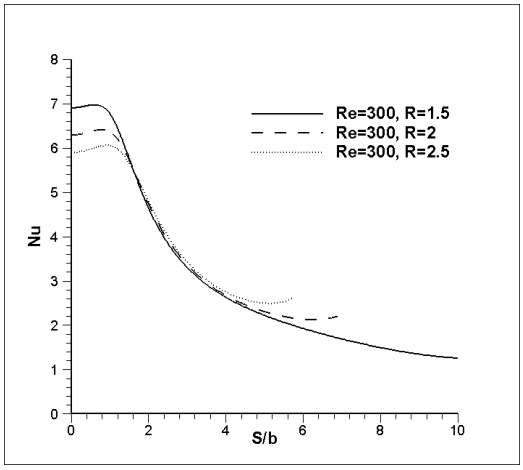

Fig. 7 Comparison for Nusselt number distribution over concave impinging plate at different radius ratios

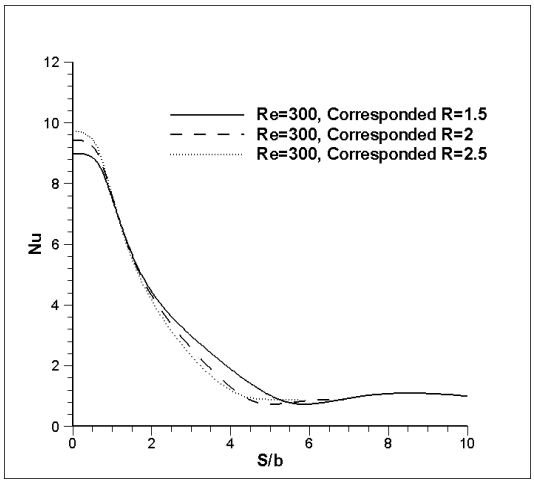

Fig. 8 Comparison for Nusselt number distribution over convex impinging plate at different radius ratios

IV. Conclusion

Lack of the comprehensive and accurate results for laminar impinging jets upon curved surface are inspirations for this study, so a numerical investigation is done to investigate the effect of the curvature on heat transfer at this flow configuration. A compressible finite volume method is used to simulate flow behavior at two different Reynolds numbers and at the fixed dimensionless nozzle to impinging plate distance. A wall that is positioned at the same level with the nozzle's exit confines flow. Three different shapes: concave, convex and flat plates are chosen for impinging plate to demonstrate the effect of curvature on the flow behavior also various curvatures are examined in the curved plate cases. Results show that the Nusselt number is increased by increasing Reynolds number. Indeed, Stagnation region's Nusselt number is enhanced by increasing curvature on convex cases due to thinner formed thermal boundary layer at this region. On the contrary, Nusselt number is reduced by increasing curvature over concave plate at stagnation region. Previous results underestimate the effect of curvature on the stagnation region. Based on Kayansayan results [10] , curvature effects does not alter distribution of Nusselt number very much at the stagnation region and little dominant effect of curvature is presented at the downstream of that region. In addition, from quantitative point of the view, reference [10] results contradict logically with other published results. In spite of the dubious previous results, it is shown at this study that Nusslet number is affected seriously by curvature at stagnation region and downstream of that region. Finally, the highest stagnation region's Nusselt number at convex surface and the lowest value for concave plate's Nusselt number at that region are remarkable conclusion for the present study.

References

[1] Viskanta, R., "Heat Transfer to Impinging Isothermal Gas and Flame Jets," *Experimental Thermal and Fluid Science*, Vol. 6, pp. 111-134, 1993.

[2] Gardon, R., and Akfirat, J. C., "The Role of Turbulence in Determining the Heat transfer Characteristics of Impinging Jets," *Int. J. Heat Mass Transfer*, Vol. 8, pp. 1261-1272, 1965.

[3] Chiriac, V. C., and Ortega, A., "A Numerical Study of the Unsteady Flow and Heat Transfer in a Transitional Confined Slot Jet Impinging on an Isothermal Surface," *Int. J. Heat Mass Transfer*, Vol. 45, pp. 1237-1248, 2002.

[4] Park, T.H., Ghoi, H.G., Yoo, J.Y., and Kim, S.J., "Streamline Upwind Numerical Simulation of Two-Dimensional Confined Impinging Slot Jets," *Int. J. Heat Mass Transfer*, Vol. 46, pp. 251-262, 2003.

[5] Lee, H.G., Yoon, H.S., Ha, M.Y., "A Numerical Investigation on the Fluid Flow and Heat Transfer in the Confined Impinging Slot Jet in the Low Reynolds Number Region for Different Channel Heights," *Int. J. Heat Mass Transfer*, Vol. 51, pp. 5055-4068, 2008.

[6] Lee, D., Park, H. J., and Ligrani, P., "Mill scale Confined Impinging Slot Jets: Laminar Heat Transfer Characteristics for an Isothermal Flat Plate," *Int. J. Heat Mass Transfer*, Vol. 55 pp. 2249-2260, 2012.

[7] Rady, M., and Arquis, E., "Heat Transfer Enhancement of Multiple Impinging Slot Jets with Symmetric Exhaust Ports and Confinement Surface Protrusions," *Applied Thermal Engineering*, Vol. 26, pp.1310-1319, 2006.

[8] Kubacki, S., and Dick, E., "Simulation of Plane Impinging Jets with k-w Based Hybrid RANS/LES Models," *Int. J. Heat Mass Transfer*, Vol. 31, pp. 862-878, 2010.

[9] Jaramillo, J. E., Trias, F. X., Gorobets, A., Perez-Segarra, C. D., and Oliva, A., "DNS and RANS Modeling of a Turbulent Plane Impinging Jet," *Int. J. Heat Mass Transfer*, Vol. 55 pp. 789-801, 2012.
[10] Kayansayan, N., and Kucuka, S., "Impingement Cooling of a Semi-Cylindrical Concave Channel by Confined Slot-Air-Jet," *Experimental Thermal and Fluid Science*, Vol. 25, pp. 383-396, 2001.
[11] Rahman, M. M., and Hernandez, C. F., "Transient Conjugate Heat Transfer from a Hemispherical Plate during free Liquid Jet Impingement on the Convex Surface," *Heat and Mass Transfer*, Vol. 47, pp. 69-80, 2011.
[12] Choi, M., Yoo, H. S., Yang, G., Lee, J. S., and Sohn, D. k., "Measurements of Impinging Jet Flow and Heat Transfer on a Semi-Circular Concave Surface," *Int. J. Heat Mass Transfer*, Vol. 43 pp. 1811-1822, 2000.
[13] Yang, Y. T., Wei, T. C., and Wang, Y. H., "Numerical Study of Turbulent Slot Jet Impingement Cooling on a Semi-Circular Concave Surface," *Int. J. Heat Mass Transfer*, Vol. 54 pp. 482-489, 2011.
[14] Cornaro, C., Fleischer, A.S., and Goldestein, R.J., "Flow Visualization of a Round Jet Impinging on a Cylindrical Surfaces," *Experimental Thermal and Fluid Science*, Vol. 20 pp. 66-78, 1999.
[15] Liou, M. S., "A Sequel to AUSM: AUSM+," *Journal of Computational Physics*, Vol. 129, pp. 364-382, 1996.